Title	Synergistic effects on band gap-narrowing in titania by codoping from first-principles calculations
Author(s)	Long, Run; English, Niall J.
Publication Date	2010-02-12
Publication information	Chemistry of Materials, 22 (5): 1616-1623
Publisher	ACS Publications
Link to publisher's version	http://dx.doi.org/10.1021/cm903688z
This item's record/more information	http://hdl.handle.net/10197/2720
DOI	http://dx.doi.org/10.1021/cm903688z

Synergistic effects on band gap-narrowing in titania by codoping from first-principles calculations

The SEC Strategic Research Cluster and the Centre for Synthesis and Chemical

Biology, Conway Institute of Biomolecular and Biomedical Research, School of

Chemical and Bioprocess Engineering, University College Dublin, Belfield, Dublin 4,

Ireland

Run Long and Niall J. English[a]

Abstract: The large intrinsic band gap in TiO_2 has hindered severely its potential application for visible-light irradiation. In this study, we have used a passivated approach to modify the band edges of anatase-TiO_2 by codoping of X (N, C) with transition metals (TM=W, Re, Os) to extend the absorption edge to longer visible-light wavelengths. It was found that all the codoped systems can narrow the band gap significantly; in particular, (N+W)-codoped systems could serve as remarkably better photocatalysts with both narrowing of the band gap and relatively smaller formation energies and larger binding energies than those of (C+TM) and (N+TM)-codoped systems. Our theoretical calculations provide meaningful guides for experiments to develop more powerful visible-light photocatalysts.

---

[a] Corresponding author. Electronic Mail: niall.english@ucd.ie

1.   Introduction

Titania (TiO$_2$)-based photocatalysts have received intense attention as promising photocatalytic materials for the decomposition of organic pollutants present in water or air [1]. However, their universal use is restricted to ultraviolent light ($\lambda < 385$ nm) due to the wide band gap of titania (~3.2 eV for anatase). Further, photoexcited electron-hole pairs tend to recombine relatively easily in TiO$_2$. Both of these factors limit possible applications in photocatalytic materials design. Therefore, it is highly desirable to extend the optical absorption of TiO$_2$-based materials to the visible-light region with a low photo-generated electron-hole recombination rate.

In general, doping is one of the most effective approaches to extend the absorption edge to the visible-light range. For example, N-doped TiO$_2$ is considered to be a promising photocatalyst, and it has been investigated widely, both by experimental and theoretical methods [2]. However, due to strongly localized N 2p states at the top of valence band [3], the photocatalytic efficiency of N-doped TiO$_2$ decreases because isolated empty states trap an appreciable proportion of photo-excited electrons and reduce photo-generated current [4]. Besides N-doped TiO$_2$, C-doped TiO$_2$ also shows photocatalytic activity under visible-light [5]. On the other hand, transition metal doping can also promote photocatalytic efficiency, but this is hindered also by the presence of carrier recombination centers and the formation of strongly localized d states in the band gap, which serves to reduce carrier mobility substantially [6]. Recently, Gai et al. [7] proposed using a passivated codoping approach, consisting of nonmetal and metal elements, to extend the TiO$_2$ absorption edge into the visible light

range. Because defect bands are passivated, it is highly likely that they will be less effective as carrier recombination centers [8]. Recent experiments have reported that the addition of W to N-doped TiO_2 can increase photocatalytic activity under visible-light irradiation significantly [9, 10]. Our theoretical calculations on (N+W)-codoped anatase suggest that a continuum band is formed at the top of the valence band, and that W 5d orbitals locate below Ti 3d states at the bottom of conduction band, which narrows significantly the band gap and enhances visible light absorption [11]. To the best of our knowledge, this study [11] was the first theoretical explanation of how (N+W)-codoped anatase possesses such high photocatalytic activity. To find even more effective photocatalyst materials, one may perform further theoretical calculations of codoping with non-metal and metal elements to guide future experimental work in solar energy materials design.

In this study, we have used a passivated codoping approach to search for appropriate dopants to narrow the band gap of anatase which do not induce gap states, based on first-principles calculations. This aim is to avoid defect states which act as effective carrier recombination centers. In the analysis of the band structures of codoped anatase, it was found that although (C+TM) (TM=W, Re, Os)-codoped systems narrow the band gap slightly larger than (N+TM)-codoping cases, (N+W)-codoped TiO_2 is the more promising photocatalyst due to the narrowing of its band gap and the relatively small formation energies and large binding energies.

2.   **Methodology**

All of the spin-polarized DFT calculations were performed using the projector augmented wave (PAW) pseudopotentials as implemented in the Vienna ab initio Simulation Package (VASP) code [12, 13]. The Perdew and Wang parameterization [14] of the generalized gradient approximation (GGA) [15] was adopted for the exchange-correlation potential. The electron wave function was expanded in plane waves up to a cutoff energy of 400 eV and a Monkhorst–Pack k-point mesh [16] of 4 × 4 × 4 was used for geometry optimization [17, 18] and electronic property calculations. Both the atomic positions and cell parameters were optimized until residual forces were below 0.01 eV/Å. It is well known that GGA underestimates the band gap of TiO_2 significantly (2.0 eV vs. anatase 3.2 eV experimental value). Here, we include the on-site Coulomb correction for the Ti 3d states, the so called GGA + U method [19], which can partially improve the prediction of the band gap. Here, U = 5.3 eV for Ti, which is in agreement with the optimal value (5.5±0.5eV) [20, 21]; using this, the calculated band gap of pure anatase was 3.11 eV, which agrees well with the experimental value of 3.20 eV. A variety of U values (1.0, 2.0, 3.0, and 4.0 eV) were applied to the dopants. The calculated results for U=1.0 and 2.0 eV were found to yield a qualitatively wrong metallic ground state as in the standard GGA calculations for W, and Os, and the once the U value was increased to 3.0 eV, the behavior of W- and Os-doped TiO_2 exhibited appropriate semiconductor characteristics. For Re-doped TiO_2, band gap is not particularly dependent on the U value. Therefore, a moderate value 0f U = 3.0 eV has been applied to TM 5d states,

_2 [22].

The relaxed (2 × 2 × 1) 48-atom anatase supercell was used to construct doped systems. Single O and Ti atoms were replaced by single X (N, C) and TM (W, Re, Os) atoms, respectively. The codoped systems were created by simultaneous substitution of an O atom by an X (N, C) atom and a Ti atom by a TM (W, Re, Os) atom. In principle, the three 5d transition metal elements W, Re and Os served as n-type dopants and nonmetal elements N, C as p-type dopants. It was found that formation of adjacent metal-nonmetal element pairs is more energetically favorable with respect to other configurations. For clarity, we have listed the total energies differences between X-TM nearest-neighbor (*1nn*), the second nearest-neighbor (*2nn*) and largest-distance (*Lnn,* one dopant in the center of the supercell with the other in a corner) doped systems in Table 1. Here we set the *1nn* total energies as zero eV. It shows that almost all of the energy differences are over 0.5 eV for all systems. We also used a 108-atom supercell to test the energy differences of all the doped systems between *1nn* and *Lnn* and they confirmed the results from 48-atom calculations. Therefore, we will select the lowest-energy structures to examine their electronic properties. The supercell system and dopant sites are shown in Fig. 1.

3.   Results and discussion

3.1 Monodoping in anatase

In this section, our main concerns are to investigate the relative difficulty for single-X (N, C) and TM (W, Re, Os) ions to incorporate into the lattice and how to

engineer the band edges appropriately. Hence, we first calculated the dopant

formation according to equations. (1) and (2) below

$$E_{form} = E(X @ O) - E(TiO_2) - \mu_X + \mu_O \tag{1}$$

$$E_{form} = E(TM @ Ti) - E(TiO_2) - \mu_{TM} + \mu_{Ti} \tag{2}$$

where the $E(X @ O)$ and $E(TM @ Ti)$ are the total energies containing impurities (X=

N, C; TM=W, Re, Os) and $E(TiO_2)$ is the total energy of the pure supercell. The

formation energies for the different doped systems are considered in this work as a

function of the oxygen chemical potential (μ_O), which is a parameter that

characterizes the oxygen environment during synthesis [23-25]. The environment acts

as a reservoir, which can give or take any amount of oxygen without changing its

temperature and pressure [26]. Low values of μ_O correspond to O-poor conditions

while high values of μ_O correspond to O-rich conditions. By referencing μ_O to the

energy of an O atom in the O$_2$ molecule ($\mu_O = \frac{1}{2}\mu(O_2) + \mu'_O$), here we take

$-4eV \le \mu'_O \le 0eV$, where the value $\mu'_O = 0$ corresponds to the O-rich limit whereas

$\mu'_O = -4$ eV is approximately half of the enthalpy of formation of anatase TiO$_2$ (our

calculated value is 9.98 eV in comparison to an experimental value of 9.8 eV) [27].

The chemical potential of a Ti atom, μ_{Ti}, is calculated from $\mu_{Ti} = \mu(TiO_2) - 2\mu_O$.

For C and N, we used fixed values of the chemical potentials μ_C and μ_N and

calculated these from the formulae $\mu_C = \mu(CO_2) - \mu(O_2)$ and $\mu_N = \frac{1}{2}\mu(N_2)$. Here,

the molecular species were contained in periodic cells large enough to avoid

molecule-molecule interactions. Although a variety of N dopant sources have been

used in different experiments, such as NH$_4$Cl [28], (NH$_2$)$_2$CO [29], and N ions [30], it

6

configuration of N_2 to calculate nitrogen's chemical potential by many authors [25, 31]. Furthermore, this avoids the introduction of any other impurity atoms into the TiO_2 lattice besides the dopant sources themselves. On the other hand, CO_2 has usually been used to estimate carbon's chemical potential [24]. Similarly, the chemical potentials for W (μ_W), Re (μ_{Re}) and Os (μ_{Os}), were also fixed and calculated from the formulae $\mu_W = \mu(WO_3) - \frac{3}{2}\mu(O_2), \mu_{Re} = \mu(ReO_2) - \mu(O_2)$ and $\mu_{Os} = \mu(OsO_2) - \mu(O_2)$, respectively. The stability diagram for single-N, C and TM (W, Re, Os) doped TiO_2 is reported in Figure 2. For N- and C-doped TiO_2, the values of formation energies agree well with previous theoretical work [24, 25], indicating that our calculated method is reasonable. Figure 2a suggests that: 1) X (N, C) occupies the O site preferentially under Ti-rich conditions while possessing a high formation energy under O-rich conditions; 2) TM (W, Re, Os) may be substituted relatively easily under O-rich conditions, but it is more difficult under Ti-rich conditions.

Secondly, we investigated how to modify the band gap of TiO_2. Therefore, a knowledge of the characteristics of band edges in pure TiO_2 is needed. The density of states (DOS) and projected DOS (PDOS) of pure anatase are plotted in Figures 3 a & a'. It shows that the top of valence band is composed mainly of O 2p states and the bottom of conduction band is dominated by Ti 3d states. Therefore, to modify the valence band edge (*i.e.*, p-type doping), one should choose a different p orbital energy relative to the O atom, and to modify the conduction band edge (n-type doping),

different d orbital energies relative to the Ti atom should be selected.

For N and C dopants, these introduce acceptor states above the VBM, as one might expect. Further, C 2p acceptor states [cf. Figures 3 b&b'] lie deeper inside the gap than those of N 2p acceptor states [cf. Figures 3 c&c'] because the C 2p orbital energy is higher than that of N 2p. Replacement of Ti atoms by transition metals, W, Re, and Os, results in the largest influence occurring at the conduction band edge and gap states, respectively. The position of the donor state near the CBM depends on the d orbital energy of the dopants. Our calculated results show that W@Ti and Re@Ti substitution creates shallow levels below the Ti 3d states while Os@Ti substitution induces deep levels in the gap. Certainly, when Ti is replaced by W, Re, the impurity levels resonate with the conduction band. However, these monodoped systems either create impurities states (for C and Os) which may act as recombination centers, thereby reduce photo-efficiency, or narrow slightly the band gap of TiO_2 (for W and Re), which extends the visible-light absorption edge marginally. To investigate if the differences in electronic properties between Re- and Os-doped TiO_2 may be rationalized from the bond characteristics, we plotted the electron localization function (ELF) in Figure 4 at the (100) surface of bulk anatase for these three doped systems. The ELF is a scalar continuous function bounded between 0 and 1, and the value of 1 indicates that electrons are fully localized and 0 implies that electrons are fully delocalized or that there is no electron in that place. So the value between 0 and 1 indicates the probability of the formation of an electron-gas-like pair [32]. Figure 4 shows that the degree of electron localization is in the order W > Re > Os, which

implies that Os-O covalent bonds [cf. Figure 4(c)] are stronger than W-O ionic bonds [cf. Figure 4 (a)] and Re-O covalent bonds [cf. Figure 4(b)] so that the extent of hybridization is in the order O-W < O-Re < O-Os, which coincides with characteristics evident in the DOS.

3.2   Synergistic effects of codoping in anatase

We propose to codope anatase with donor-acceptor pairs to reduce the formation energy and to narrow the band gap further. Therefore, we calculated the formation energy for (X+TM)-codoped system, *i.e.* (N+W), (N+Re), (N+Os), (C+W), (C+Re), and (C+Os), according to eqn. (3)

$$E_{form} = E(TM@Ti + X@O) - E(TiO_2) - \mu_X - \mu_{TM} + \mu_O + \mu_{Ti} \tag{3}$$

where $E(TM@Ti + X@O)$ is the total energy of the codoped system. The formation energies are also summarized in Table 1. The results show that codoping of X (N, C) with TM (W, Re, Os) reduces the formation energies significantly with respect to N and C monodoping under O-rich conditions, which corresponds to the usual growth conditions for synthesis samples in experiments. This indicates that codoping is beneficial for C or N introduction into the titania lattice. Hence, one could select W, Re, and Os to act as the codopants with N or C to favor the incorporation of N or C into the titania lattice in experiments. Furthermore, (N+TM)-codoped systems have lower formation energies than (C+TM)-doped TiO_2, which means that synthesis of the (N+TM) samples is relatively easier than the (C+TM) case.

Before we study the passivation effect on the band gap of TiO_2 via X-TM codoping,

one needs to consider the stability of defect pairs. Therefore, we calculated the defect

pair binding energy [33] according to eqns. (4) and (5)

$$E_b = E(TM@Ti) + E(C@O) - E(TM@Ti + C@O) - E(TiO_2) \qquad (4)$$

$$E_b = E(TM@Ti) + E(N@O) - E(TM@Ti + N@O) - E(TiO_2) \qquad (5)$$

Positive E_b values indicate that the defect pairs tend to bind to each other and are

stable. The calculated binding energies for the (C+W), (C+Re), (C+Os), (N+W),

(N+Re), and (N+Os) pairs are 3.15, 0.65, 3.94, 2.64, 0.23, and 2.54 eV, respectively,

indicating that C-W, C-Os, N-W, and N-Os impurities pairs are significantly stable

relative to the isolated dopants. Furthermore, these binding energies are comparable

with the reported result of Gai et al. [7]. However, the values of binding energy for

C-Re and N-Re impurities pairs are not large enough and may possibly be broken up

at high temperatures during the synthesis process. To confirm this, we also calculated

the binding energies with a 108-atom supercell using a $2 \times 2 \times 2$ k-mesh. The

corresponding values are 2.84, 0.50, 4.56, 2.28, 0.20, and 2.55 eV, respectively,

indicating that the binding energies from the 48-atom system is reasonable. The large

binding energy results arises from charge transfer from donor to acceptor and the

strong associated Coulomb interaction is due to interactions between positively

charged donors and negatively charged acceptors. The ELF is plotted in Figure 5 at

the (100) surface of bulk anatase for these three doped systems and the Bader charges

are summarized in Tables 2 and 3 [34, 35]. Here, the partial optimized geometries are

presented in Figure 6 to compare with Tables 2 and 3. Figure 5 shows that C-W and

C-Re bonds exhibit ionic behavior while C-Os shows covalent characteristics. Table 2

shows that the C ion has a charge of -1.20 |e| for C@O monodoping, while it is -2.60 |e| for (C+W)-codoping, with more electrons transferring from the W and adjacent Ti atoms to the C ion. The bond length of C-W is 1.868 Å, which is shorter than that of the C-Ti length of 2.196 Å for C@O doping, indicating further that a strong C-W bond forms. For (C+Re), the optimized C-Re bond length is only 1.624 Å, shorter than that of C-W and significantly shorter than that of C-Ti. Therefore, a much stronger interaction between the C and Re ion takes place. For the (C+Os) system, the C-Os bond behavior is different from C-W and C-Re (cf. Figure 5) such that the formation of a covalent C-Os bond takes place through sharing of electrons between Os and C. The Bader charges also confirm this result, in which the C ion has a charge of -2.74 |e|. This method could be also employed to analyze the (N+TM) system.

Secondly, we have examined synergistic effects on narrowing the band gap of TiO_2 by codoping X (N, C) with TM (W, Re, Os). Hence, the calculated DOS and PDOS for these six systems, compared to the results with that of pure TiO_2, are shown in Figure 7. It may be seen that the reduction in band gap caused by codoping is very significant with respect to that observed in the corresponding X (N, C) and TM (W, Re, Os) monodoped cases, leading to a large reduction of band gap in these doped systems.

For (N+W) codoped system (cf. Figures 7 a&a'), identifying the formation of a continuous band of hybridized N2p-O2p states, which consists of the valence band edge and W5d orbitals dominating the conduction band edge, leading to a significant band gap reduction of about 1.37 eV [11]. It means (N+W) codoped TiO2 is a

effective photocatalysts to absorb visible-light. Then, we examine the other two (N+TM)-codoped systems. (N+Re) (cf. Figures 7b&b') and (N+Os) (cf. Figures 7c&c') possess much smaller band gaps than those of both pure anatase and the (N+W) system. However, there are some shortcomings in them. Firstly, the binding energy of (N+Re) system is so small that it is easily departed during synthesis process. Secondly, some empty states located in the band gap of (N+Os) system that can act as recombination centres and reduce phonon absorption efficiency. Although these two codoped systems extend substantially the absorption edge to longer visible-light ranges, it's expected they are not effective and applied photocatalysts because of either unstable or low efficiency.

Compared to (N+TM)-codoped systems, (C+TM) exhibits much better effects on band gap narrowing, which may be due to deeper C acceptor energy levels than those of N, and a much stronger interaction between C and TM atoms. For the (C+W) codoped system (cf. Figures 7 d & d'), the band gap is reduced by about 1.41 eV with formation of isolated band above VBM with an value of 0.83 eV and CBM down-shifting by about 0.37 eV, which is different from the (N+W) system. Like (N+W)-codoped titania [11], a C2p-W5d hybridized band is formed, which renders the hybridization between C 2p and O 2p stronger than C monodoping, giving rise to a fully occupied band above the top of valence band edge. At the same time, partial W 5d states are located at the edge of the conduction band, and importantly, the isolated states disappear and a continuum-like band is formed. This finding is very similar to our previous work on (N+Ta)-codoped TiO_2 [36]. Obviously, incorporation of W into

C-doped TiO$_2$ changes the character of C 2p orbitals from isolated midgap states to C 2p states mixed with O 2p states above the top of the valence band and conduction band edge consisting of W 5d itself. However, its formation energy is nearly double that of the (N+W) case and therefore it would not be easily synthesized experimentally under either O-rich or Ti-rich conditions.

The (C+Re) codoped system (cf. Figures 7 e&e') reduces the band gap significantly by about 1.89 eV, with formation of a fully occupied band above the VBM about 0.4 eV and CBM down-shifting by 1.43 eV, which is different from the (C+Os) codoped cases (cf. Figures 7 f & f'). The band gap of (C+Os) case narrows less than (C+Re) but produces gap states, which are partially occupied. This implies that the (C+Os)-codoped system is not as promising as a possible photocatalytic material due to the existence of recombination centers. However, the small binding energy of (C+Re)-codoped anatase leads this system to be unstable at high temperatures.

Briefly, considering the findings for band gap narrowing, formation energies, and binding energies, it seems that (N+W) and (C+W) should be promising candidates for photocatalytic materials under visible light irradiation. Therefore, we have plotted the DOS and PDOS for these doping cases (N, C and W as far apart as possible, i.e. the *Lnn* configuration) in Figure 8. For the (N+W) system (cf. Figures 8 a&a'), the value of band gap narrowing is about 1.11 eV, which is smaller than that of 1.37 eV with the formation of an N-W pair. Furthermore, the impurity band locates about the VBM, which is very different from Figure 7a due to no passivation effect. On the other hand, the (C+W) system (cf. Figures 8 b&b') exhibits some unoccupied states locating at

band gap acting as recombination centers. This is quite different behavior from Figure 7d, in which there are no such unoccupied states which may serve to accommodate recombination centers.

To compare different dopant concentration effects on electronic structure, we selected the best (N+W) and (C+W)-codoped systems and calculated their DOS and PDOS using the GGA+U method with a 108-atom supercell, as shown in Figure 9. For comparison, we have also presented the DOS and PDOS of the pure 108-atom anatase supercell. The electronic structures of the (N+W)-codoped case (cf. Figures 9 (a)&(a')) exhibit two obvious different characteristics compared with the 48-atom supercell (cf. Figure 7 (a)&(a')). Firstly, the gap narrowed less. Secondly, there is formation of a fully-occupied continuum-like band above the VBM. Nevertheless, this still shows excellent potential band gap behavior to absorb more visible light. On the other hand, (C+W)-codoped TiO_2 (cf. Figures 9(b)&(b')) has similar electronic properties with respect to its 48-atom supercell analogue, except a comparatively smaller band gap reduction due to the lower doping concentration. Therefore, this also serves as a promising photocatalytic material under visible-light irradiation independent of consideration of formation energy.

C may also certainly occupy interstitial sites, in particular, under O-rich conditions [21]. Therefore, we consider three configurations of C locating at interstitial sites and TM (W, Re, Os) locating at Ti sites. Partial views of the geometry-optimized structures are shown in Figures 6(g)-(i); the C-W, C-Re, and C-Os bond lengths were 1.995, 1.938, and 1.962 Å, respectively. The formation energies were calculated from

the formula (6)

$$E_{form} = E(TM@Ti + C_{in}) - E(TiO_2) - \mu_X - \mu_{TM} + \mu_{Ti} \qquad (6)$$

Here, $E(TM@Ti + C_{in})$ represents the total energies of the defective systems. The formation energies are plotted in Figure 10. It shows that the values of formation energies are always high regardless of whether growth conditions are O- or Ti-rich. Therefore, it is more difficult to fabricate these codoped systems.

In conclusion, based on first-principles calculations and analysis of electronic structures, we find that although (C+TM) (TM=W, Re, Os)-codoped systems narrow the band gap to a slightly larger extent than those of (N+TM) systems, (N+TM) has more medium formation energies, which is of greater convenience for synthesis. Band gap narrowing is a highly important contribution to the enhancement of optical absorption under visible light irradiation. The calculated results suggest that codoping of N or C with TM can effectively reduce the formation energy relative to N and C monodoping and enhance the N or C concentration. The results indicate that (N+W)-codoped anatase may serve as a very promising photocatalytic material because of its relatively small formation energy and large binding energy.

15

References

(1) Hoffmann,M. R.; Martin, S. T.; Choi, W.W.; Bahnemann, D. W. *Chem. Rev.* **1995**, *95*, 69-96.

(2) Asahi, R.; Morikawa, T.; Ohwaki, T.; Aoki, K.; Taga,Y. *Science* **2001**, 293, 269-271.

(3) Irie, H.; Watanabe, Y.; Hashimoto, K. *J. Phys. Chem. B* **2003**, *107*, 5483-5486.

(4) Lin, Z.; Orlov, A.; Lambert, R. M.; Payne, M. C. *J. Phys. Chem. B* **2005**, *109*, 20948-20952.

(5) Chen, X. B.; Burda, C. *J. Am. Chem. Soc.* **2008**, *130*, 5018-5019.

(6) Mu,W.; Herrmann, J. M.; Pichat, P. *Catal. Lett.* **1989**, *3*, 73-75.

(7) Gai,Y. Q.; Li, J. B.; Li, A. S.; Xia, J. B.; Wei, S. H.; *Phys. Rev. Lett.* **2009**, *102*, 036402-036405.

(8) Ahn, K. S.; Yan,Y.; Shet, S.; Deutsch, T.; Turner, J.; Al-Jassim, M. *Appl. Phys. Lett.* **2007**. *91*, 231909-231911.

(9) Gao, B. F.; Ma, Y.; Cao, Y. A.; Yang, W. S.; Yao, J. N. J.Phys. Chem. B 2006, 110, 14391-14397.

(10) Shen, Y. F.; Xiong, T. Y.; Li, T. F.; Yang, K. Appl. Caal., B 2008, 83, 177-185.

(11) Long, R.; English, N. J. *Appl. Phys. Lett.* **2009**, *94*, 132102-132104.

(12) Kresse, G.; Hafner, J. *Phys. Rev. B* **1994**, *47*, 558-561.

(13) Kresse, G.; Furtherműller, J. *Phys. Rev. B* **1996**, *54*, 11169-11186.

(14) Perdew, J. P.; Burk, K.; Ernzerhof, M. *Phys. Rev. Lett.* **1996**, *77*, 3865-3868.

(15) Perdew, J. P.; Wang, Y. *Phys. Rev. B* **1992**, *45*, 13244-13249.

(16) Monkhorst, H. J.; Pack, J. D. *Phys. Rev. B* **1976**, *13*, 5188-5192.

(17) Davidson, E. R. *Methods in Computational Molecular Physics* edited by G.H.F. Diercksen

(18) Wilson, S. Vol. 113 *NATO Advanced Study Institute, Series C* (Plenum, New York, 1983), p. 95.

(19) Dudarev, S. L.; Botton, G. A.; Savarsov, S. Y.; Humphreys, C. J.; Sutton, A. P. *Phys. Rev. B* **1998**, *57*, 1505.

(20) Calzado, C. J.; Hernández, Sanz, J. F. Phys. Rev. B 2008, 77, 045118.

(21) Anisimov, V. I.; Korotin, M. A.; Nekrasov, I. A.; Mylnikova, A. S.;　Lukoyanov, A. V.; Wang, J. L.; and Zeng, Z. J. Phys.: Condens. Matter 2006. 18, 1695.

(22) Du, X. S.; Li, Q. X.; Su, H. B.; and Yang, J. L. Phys. Rev. B 2006, 74, 233201.

(23) Wilson, N. C.; Grey, I. E.; Russo. S. P. *J. Phys. Chem. C.* **2007**,*111*, 10915-10922.

(24) Valentin, C. Di.; Pacchioni, G.; Selloni, A. *Chem. Mater.* **2005**, *17*, 6656-6665.

(25) Finazzi, E.; Valentin, C. Di.. *J. Phys. Chem. C* **2007**, *111*, 9275-9582.

(26) Reuter, K.; Scheffler, M. *Phys. Rev. B* **2001**, *65*, 035406.

(27) *CRC Handbook of Chemistry and Physics* 87th ed.; Lide, D. R. Taylor & Francis: London, 2006.

(28) Valelntin, C. Di.; Pacchioni, G.; Selloni, A.; Livraghi, S.; and Giamello, E. *J. Phys. Chem. C* **2005**, *119*, 11414.

(29) Chi, B.; Zhao, L.; Jin, T. *J. Phys. Chem. C* **2007**, *111*, 6189.

(30) Batzill, M.; Morales, E. H.; and Diebold, U. *Phys. Rev. Lett.* **2006**, *96*, 026103.

(31) Yang, K. S.; Dai, Y.; Huang, B. B.; and Han, S. H. *J.Phys. Chem. B.* **2006**, *110*,

(32) Becke, A. D.; and Edgecombe, K. E. *J. Chem. Phys.* **1990**, *92* 5397.

(33) Li, J.; Wei, S. H.; Li, S. S.; Xia, J. B. *Phys. Rev. B* **2006**, *74*, 081201(1)-(4).

(34) Henkelman, G.; Arnaldsson, A.; Jónsson, H. *Comput. Mater. Sci.* **2006**, *36*, 354-.

(35) Sanville, E.; Kenny, S. D.; Smith, R.; Henkelman, G. *J. Comp. Chem.* **2007**, *28*, 899.

(36) Long, R.; English, J. N. *Chem. Phys. Lett.* **2009**, *48*, 175-179.

Table 1. Total energy difference of different doping systems (in eV). The total energy of nearest-neighbor configuration (*1nn*) has been set as zero.

	N+W	N+Re	N+Os	C+W	N+Re	C+Os
1nn	0	0	0	0	0	0
2nn	0.48	0.95	1.0	1.1	0.35	3.1
Lnn	0.57	1.1	1.1	1.3	0.56	3.3

Table 2 Average Bader Charges (|e|) on dopant atoms and their adjacent atoms in C-, and (C+W), (C+Re), and (C+Os)-doped TiO$_2$. Bond lengths of C-Ti and C-W, C-Re, and C-Os are also reported. The number in parenthesis denotes the number of nearest-neighbor atoms around a dopant.

	C-doped	(C+W)-doped	(C+Re)-doped	(C+Os)-doped
C	-1.20	-2.60	-2.60	-1.74
TM		4.82	2.94	0.97
O		-1.52(5)	-1.29(5)	-1.31(5)
Ti	2.69(3)	2.65 (2)	2.58(2)	2.71(2)
Bond length(Å)	2.196	1.868	1.624	1.743

Table 3 Average Bader Charges (|e|) on dopant atoms and their adjacent atoms in N-, and (N+W), (N+Re), and (N+Os)-doped TiO_2. Bond lengths of N-Ti and N-W, N-Re, and N-Os are also specified. The number in parenthesis denotes the number of nearest-neighbor atoms around a dopant.

	N-doped	(N+W)-doped	(N+Re)-doped	(N+Os)-doped
N	*-1.41*	*-2.02*	*-1.94*	*-0.74*
TM		*4.22*	*2.68*	*2.55*
O		*-1.47(5)*	*-1.31(5)*	*-1.31(5)*
Ti	*2.74(3)*	*2.72 (2)*	*2.59(2)*	*2.75(2)*
Bond length(Å)	*2.026*	*1.851*	*1.717*	*1.798*

Figure Captions

Figure 1. Supercell model for defective anatase showing the location of the dopants. The ion doping sites are marked with X (C, N) and TM (W, Re, Os). The 1nn, 2nn, and Lnn configurations correspond to the nearest-neighbor, the second-neighbor and the largest distance between X and TM atoms. The large light spheres and the small dark spheres represent the Ti and O atoms, respectively.

Figure 2 Formation energies (eV) E_{form} as a function of the oxygen chemical potential for (a) monodoped (C, N, W, Re, Os) and (b) codoped (N+W, N+Re, N+Os, C+W, C+Re, C+Os) anatase.

Figure 3 DOS for monodoped anatase compared with pure anatase and PDOS for impurity and host atoms (black for p orbital and green for d orbital). The top of the valence band for pure anatase is taken as the reference level. The dashed lines represent the Fermi level, E_F.

Figure 4 Electron localization function contour plots (ELF) on the (100) surface of bulk materials for (a) W-, (b) Re-, and (c) Os-doped anatase.

Figure 5 Electron localization function contour plots (ELF) on the (100) surface of bulk materials for (a) C-, (b) (C+W)-, (c) (C+Re), and (C+Os)-doped anatase.

Figure 6 Geometry-optimized structures for (a) (C+W)-, (b) (C+Re), (c) (C+Os) (d)

(N+W), (e) (N+Re), (f) (N+Os), (g) C in W, (h) C in Re, and (i) C in Os-doped anatase. The bond length unit is $\overset{\prime}{A}$

Figure 7 DOS of undoped anatase and (C+W), (C+Re), (C+Os), (N+W), (N+Re), and (N+Os)-codoped anatase and PDOS for impurity atoms (black for p orbital and green for d orbital) with 48-atom supercell. The top of the valence band of pure anatase is taken as the reference level. The dashed lines represent the Fermi level, E_F.

Figure 8 DOS for (N+W) and(C+W) codoped anatase compared with pure anatase and PDOS for impurity and host atoms using a 108-atom supercell (black for p orbital and green for d orbital). The top of the valence band for pure anatase is taken as the reference level. The dashed lines represent the Fermi level, E_F.

Figure 9 DOS for (N+W) and(C+W) codoped anatase (black for p orbital and green for d orbital). The top of the valence band for pure anatase is taken as the reference level (not shown here). The dashed lines represent the Fermi level, E_F.

Figure 10 Formation energies (eV) E_{form} as a function of the oxygen chemical potential for (a) C in W, (b) C in Re and (c) C in Os-doped TiO_2.
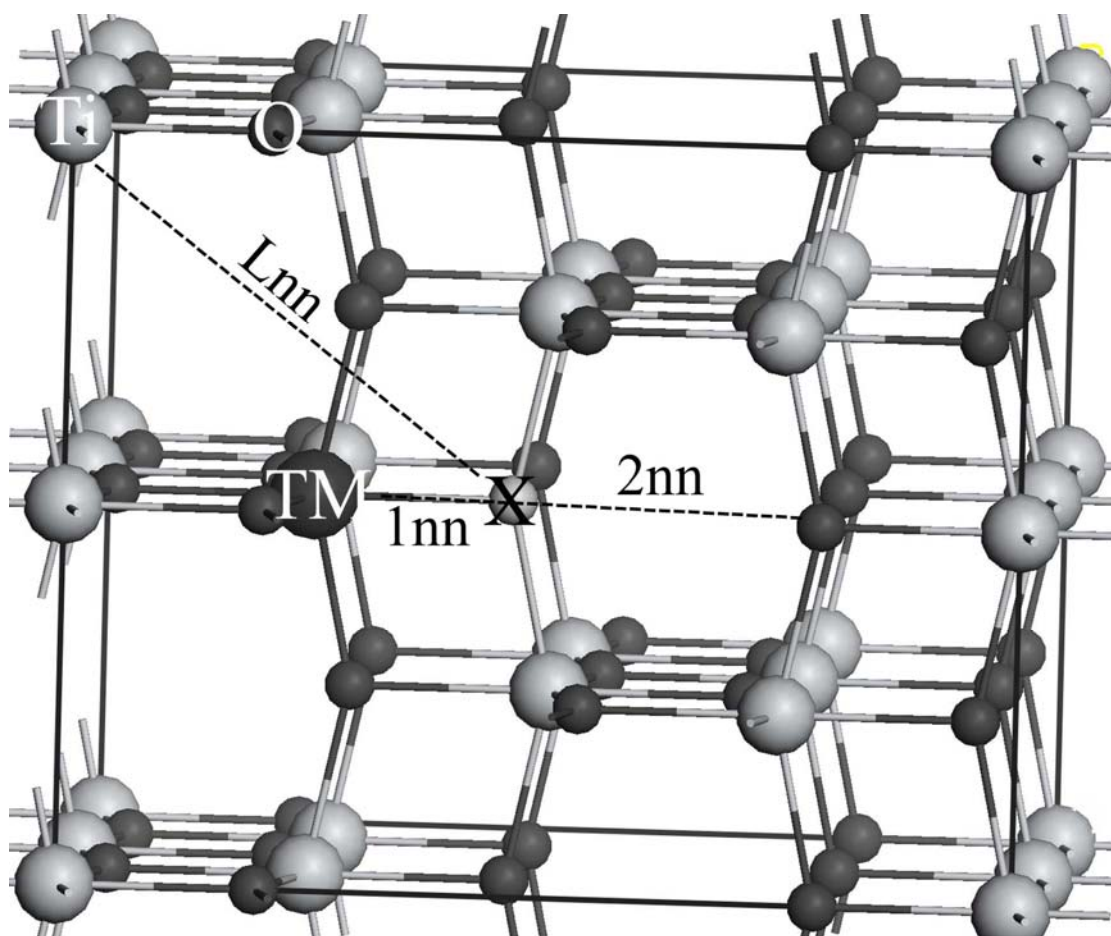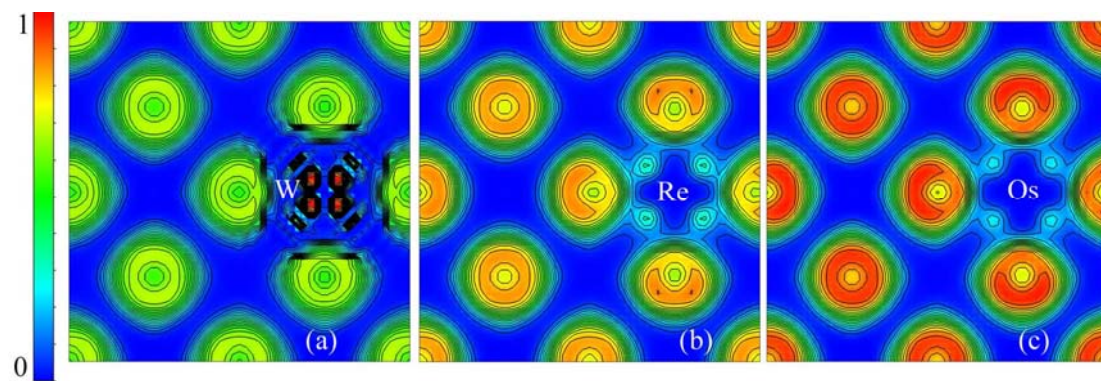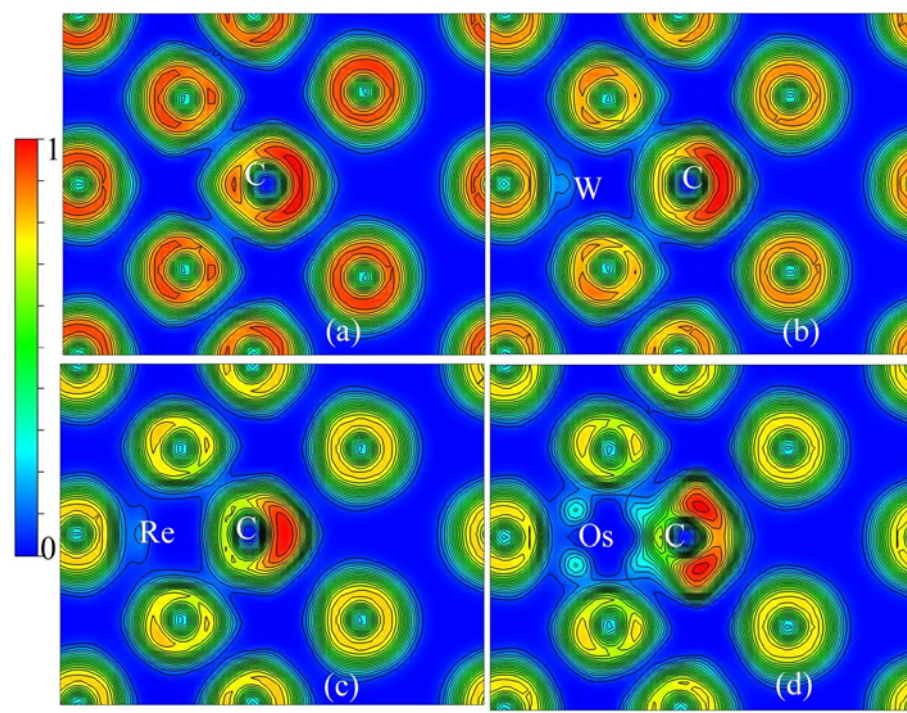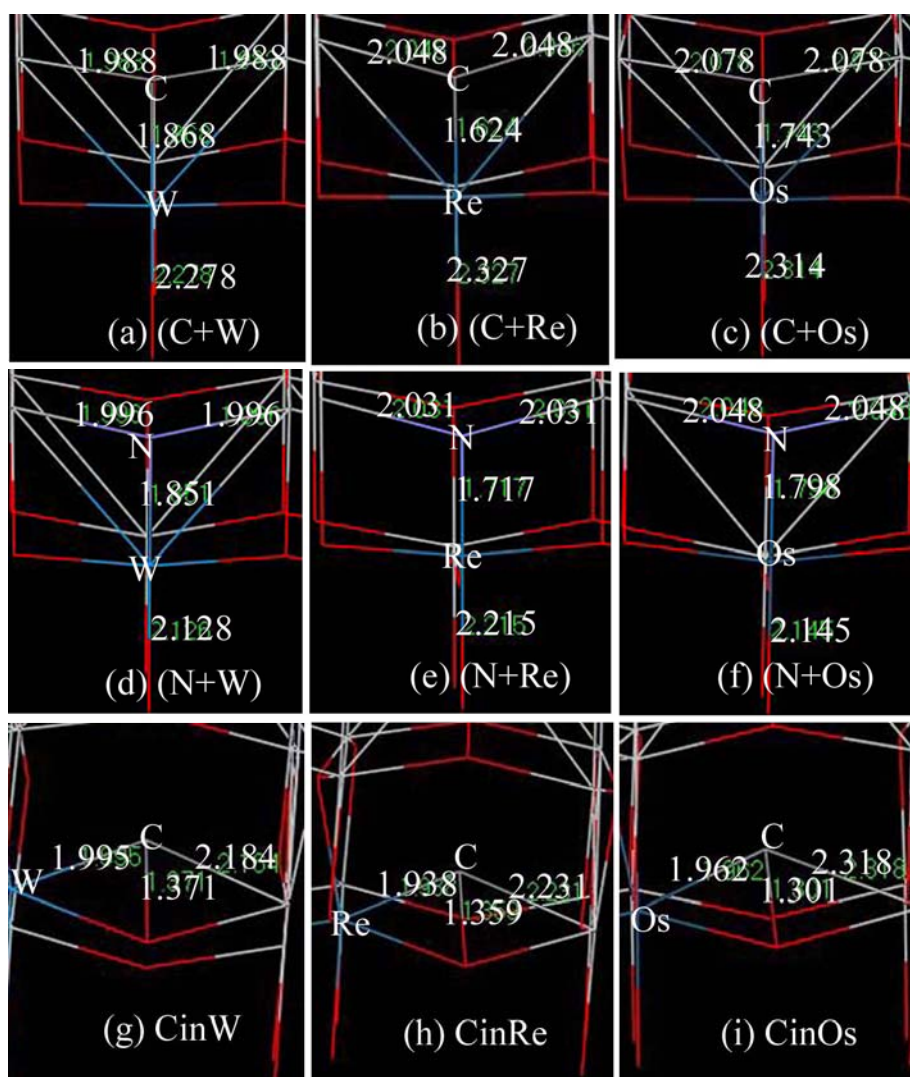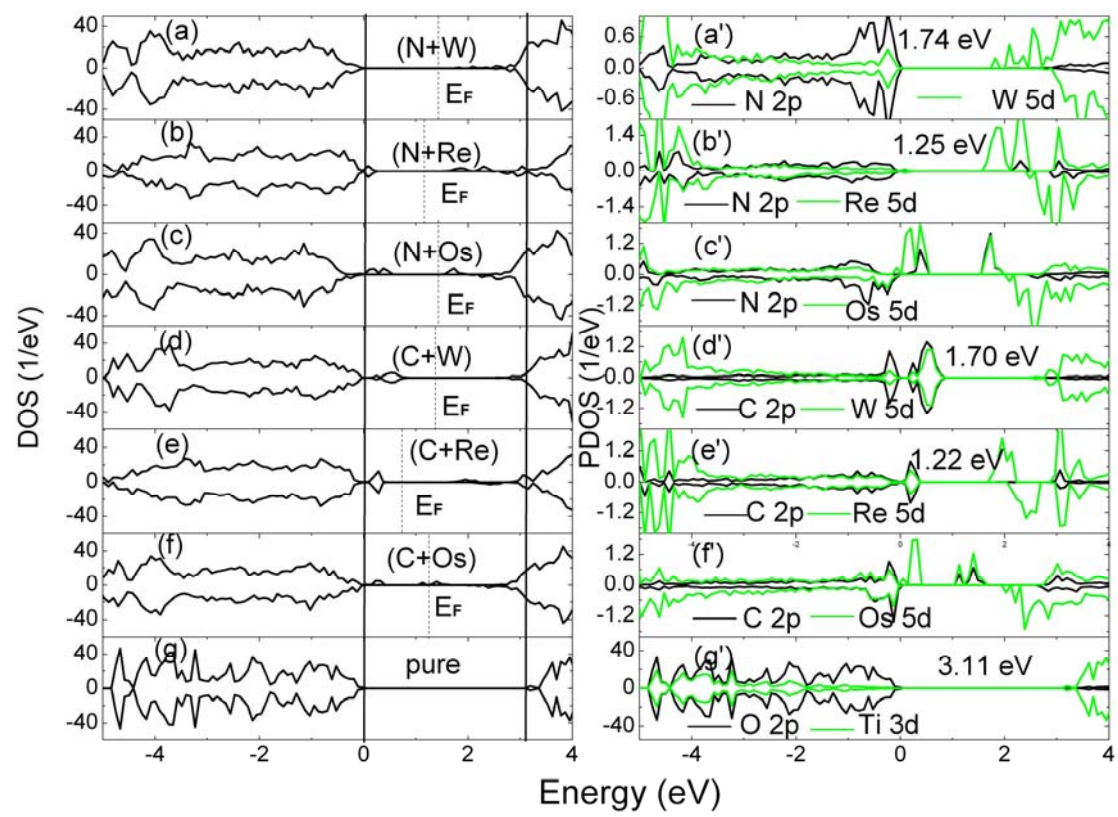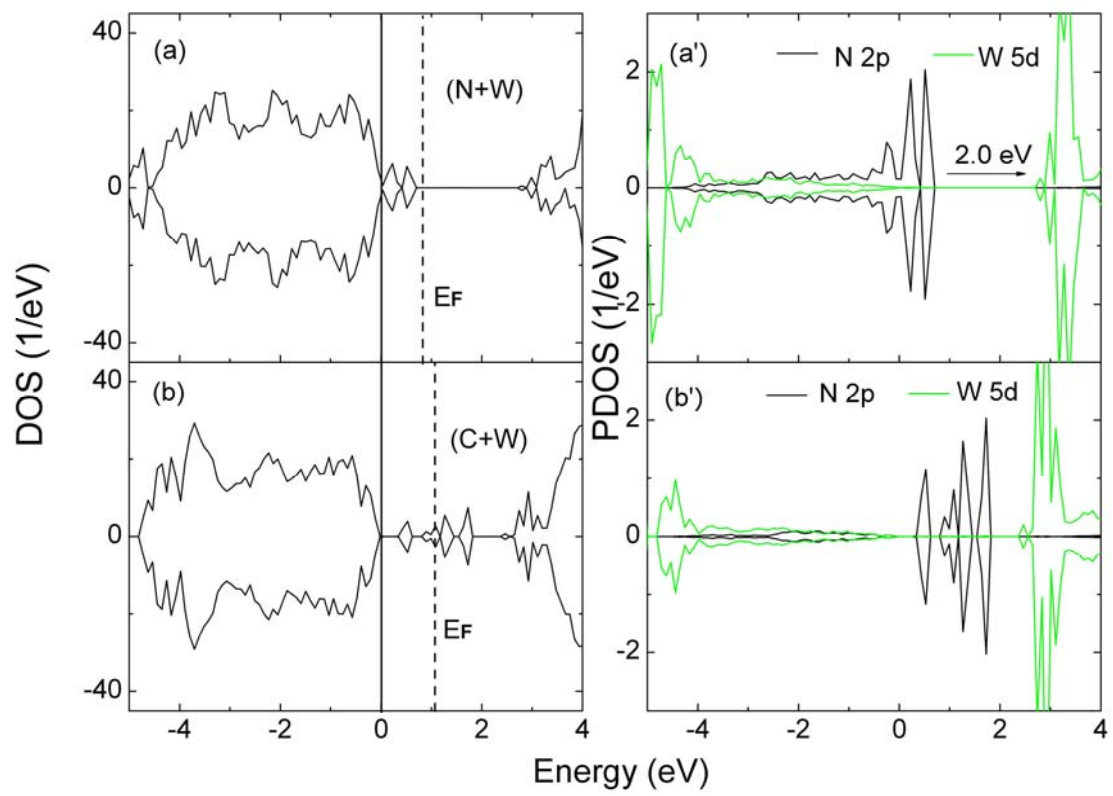
Figure 1
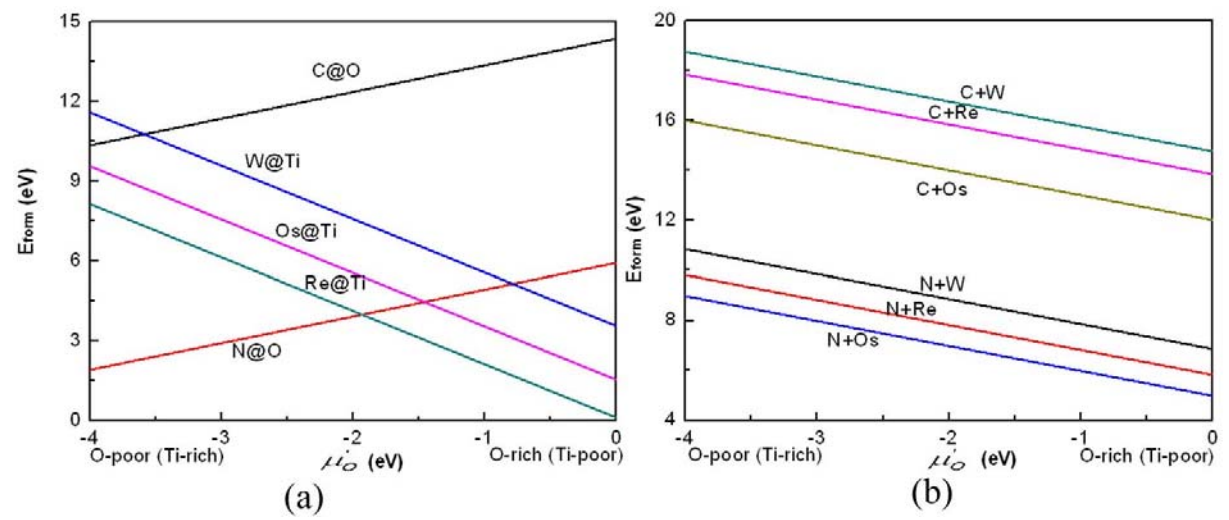
Figure 2
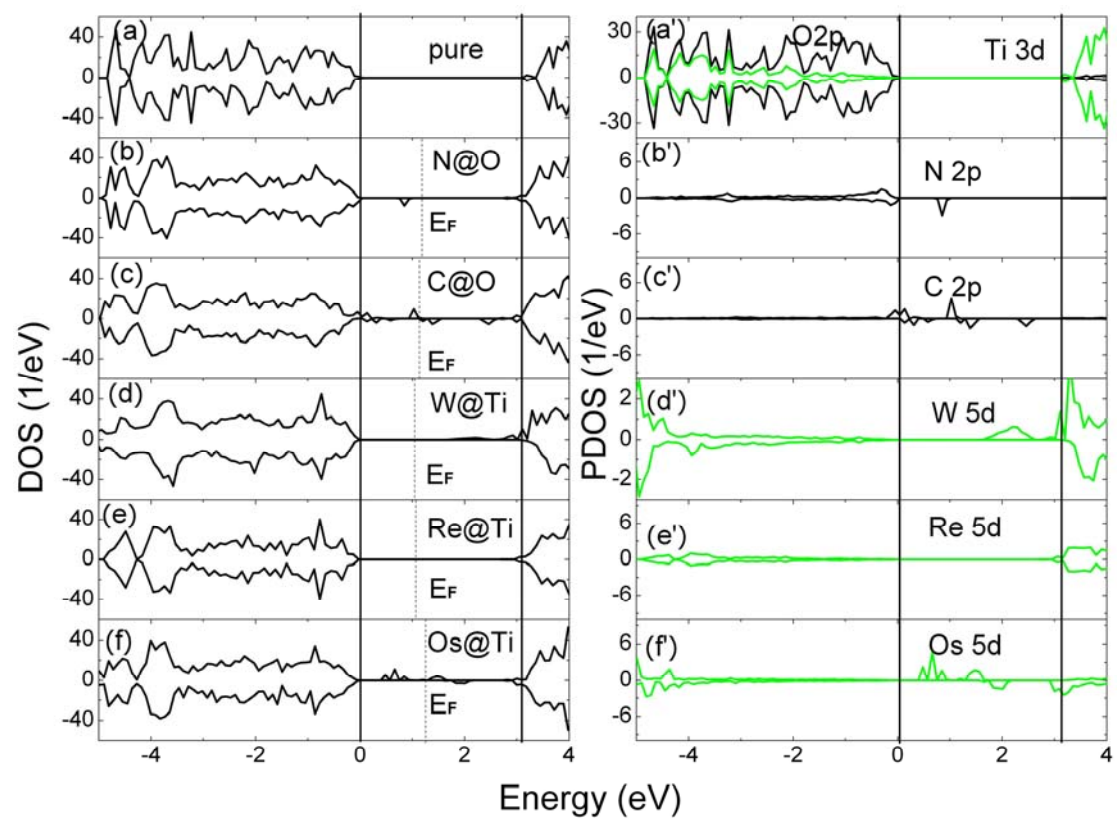
Figure 3

Figure 4

Figure 5

Figure 6

Figure 7

Figure 8

Figure 9

Figure 10